Journal of Molecular Structure 1229 (2021) 129841

Contents lists available at ScienceDirect

Journal of Molecular Structure

journal homepage: www.elsevier.com/locate/molstr

On the combination of modern sorbents with cost analysis: A review

Efstathios V. Liakos[a], Despina A. Gkika[b], Athanasios C. Mitropoulos[a], Kostas A. Matis[c], George Z. Kyzas[a,*]

[a] Department of Chemistry, International Hellenic University, Kavala, 65404, Greece
[b] Department of Physics, International Hellenic University, Kavala, 65404, Greece
[c] Department of Chemistry, Aristotle University, Thessaloniki, 54124, Greece

ARTICLE INFO

Article history:
Received 2 October 2020
Revised 17 December 2020
Accepted 22 December 2020
Available online 29 December 2020

Keywords:
Synthetic route cost
Sorption
Equilibrium
Kinetics
Heavy metals
Dyes

ABSTRACT

This review paper investigates the modern trends of sorption, presenting examples of the use of sorbents for the removal of dyes and heavy metal ions, in line with estimations of the cost fingerprint through combined calculations of raw material and energy data. The feasibility of the selected materials was explored by estimation of synthetic route cost. The examined synthetic routes include activated carbon samples derived from potato peels, coffee residues, as well as graphene oxide and chitosan. The synthesis steps and the appropriate apparatus, adsorption capacity, equilibrium parameters for the adsorption of heavy metals and dyes from aqueous solution are presented. Furthermore, the findings were compared for kinetic properties (pseudo-first, -second and -third order adsorption rate), and the costs of raw materials and energy of the selected synthetic routes were explored. A comparative study was carried out in order to evaluate the adsorption capacity of some recently published adsorbents, since their high adsorption capacity, in line with their low cost, make them very attractive and promising candidates for industrial use. The equilibrium and kinetics parameters were calculated according to the Langmuir, Freundlich and Langmuir-Freundlich (L-F) equations.

1. Introduction

Nanotechnology can be applied to the synthesis and functionalization of materials at a nanometer scale (1 nm = 10^{-9} m) [1], which then can be used in various fields as wastewater treatment (sorption process) [2], photocatalysis [3], electrodes for photochemical sensing platform [4], drug delivery [5-8], nanovaccinology [9], switchable device technologies [10], optoelectronics [11] etc.

The process of sorption, is an important and efficient technique, when used at an industrial scale. It can be used as a purification and separation technique, and thus has become a very attractive option for the wastewater treatment. There are multiple recent examples of sorption applications in literature, including: hydroxyapatite synthesized for industrial waste [12], graphene oxide [13], multiwall carbon nanotubes for emerging organic contaminants [14], different biochars and silver nanoparticles for the removal of toxic heavy metal ions (i.e. cadmium ions) [15,16].

The literature reveals that many researchers worldwide are doing research on the synthesis of novel materials for low-cost adsorption applications for decontamination [17]. Furthermore, it should be noted that the process of biosorption is another alternative technique when used for the uptake of heavy metals from dead biomass. Because this process offers an economical and feasible approach, it has gained great credibility [18,19]. The ability and effectiveness of the microbes to uptake ions of metal from aqueous solutions is a well-known phenomenon which can be achieved via several different mechanisms. In addition, the microbes have high surface area-to-volume ratio due to their small size, which allows for a large area of contact, which in turn interacts with the environment that surrounds them, including the metal effluents.

By definition, the process of sorption is a general term which is used for the description of attachment of charged species (for example ions derived from toxic metals) from an aqueous solution to a coexisting surface with solid structure. The kinetics of sorption may be verified through a lot of processes, which are independent and can act in parallel or in series; these procedures can be divided according to the following categories: bulk diffusion, intraparticle diffusion, chemical reaction (chemisorption) and transfer of external mass (film diffusion).

This review article attempts to combine the adsorption data of a set of modern materials synthesized in recent years and estimate the cost fingerprint through combined calculations of raw material and energy data.

* Corresponding author.
E-mail address: kyzas@chem.ihu.gr (G.Z. Kyzas).

https://doi.org/10.1016/j.molstruc.2020.129841
0022-2860/

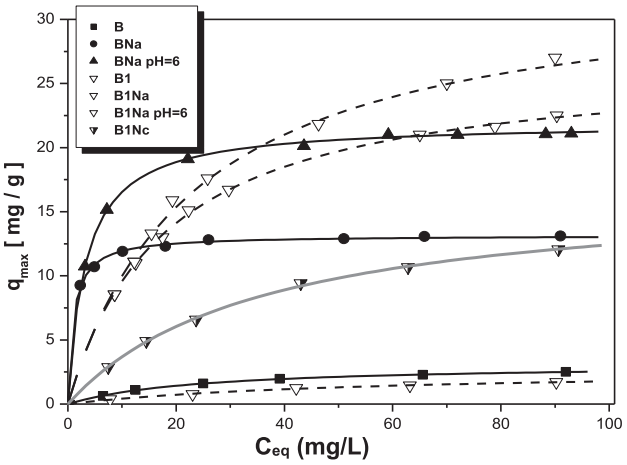

Fig. 1. Langmuir adsorption isotherms were derived from the removal of arsenate ions onto activated carbon impregnated by iron (III) oxyhydroxide nanocrystals; where 'B' is the isotherm of the initial sample, and '1' refers to the oxidized sample; in addition 'N' corresponds to iron nitrate, 'a' is used for the ammonia solution and 'c' for the ammonium carbonate, in order to make comparisons. Reproduced with permission taken by Taylor and Francis, 2013 [25].

2. Equilibrium and kinetics

The isotherm equation of Langmuir was revealed to fit in quite competently in many cases of the experimental data [20]. The isotherms of adsorption of metal oxyanions or cations, which were derived under various temperatures, concentrations of sorbent etc. are depicted through figures and tables that reveal the fitting results, as confirmed by the experimental data (equilibrium) via the isotherm of Langmuir. In the case where the values of the respective coefficient of correlation are high, they are mainly employed in order to publish a description which has satisfactory results or characteristics. Great attention should be paid to any potential error of the experimental data.

Alternatively, the isotherm of Freundlich model is extensively used in industrial scale applications. It is however inaccurate in the case of low concentration, while accurate in the case of higher concentration, due to the nature of the law of power. It was revealed that the properties of equilibrium phase do not change proportionally during the insertion of sorbent material, which could be attributed to the aggregation of solids in the case of higher loads and thus results in the decrease of effective adsorption surface [21].

The isotherm equation of Langmuir has also been found to fit well with the removal of metal ions by a cross-linked chelating resin, cadmium and a dye with a bone-meal derived apatite [22], cadmium using an activated carbon/zirconium oxide composite [23]; it should be noted that activated carbon is the most frequent used sorbent material. Apart from these two aforementioned isotherms, there are a number of other sorption isotherms that have been used in the sorption field, such as the Dubinin-Radushkevich, Tempkin, Redlich-Peterson, Sips, Toth, Khan, BET etc.; the respective equations were provided [24] in a recent review on nanomaterials as adsorbents.

Fig. 1 presents the Langmuir isotherms in the case of adsorption of arsenate. More specifically, the results for the primary and oxidized specimens of activated carbon (impregnated specimens) are presented; the materials investigation was achieved through the use of N_2 adsorption (BET), SEM, XPS, XRD, FTIR and thermal analysis [25]. The isotherms of Langmuir method, which were obtained during the study of equilibrium phase, lend extra support to the notion of a monolayer. An editorial in this field by Tien, 2007 is worth mentioning– as it was deemed rather astonishing by many researchers.

As mentioned, the kinetics of the sorption technique may be verified through various processes which are independent and can act in parallel or in series. From the category of chemical reactions, the best fit for the data under examination is often obtained by the chemical reactions of 2nd order-type; [26-28] for dyes sorbed onto mesoporous carbons, arsenates onto modified akaganeite, bisphenol A (an endocrine disruptor) onto carbonaceous materials, modified graphene oxide for mercury removal [29] and magnetic biochar composites for cadmium adsorption [30].

An appropriate magnetic adsorbent composite material is one of the most important factors to achieve a successful separation process, which in turn dominates the sensitivity and selectivity of the used technique; in fact, the method of magnetic separation has long been applied in mineral processing. Another effective solid/liquid separation technique in this field is flotation– i.e. for the loaded sorbent material [31]. Many composite materials, which are used as sorbents for sorption applications, are often synthesized (low-cost reasons) in the form of ultrafine or fine particulates. Their application should thus be in mixed-flow type equipment to prevent losses from high pressure.

The following examples deal with the uptake (and depletion) of chromates and cadmium from aqueous solutions, through the process of biosorption by using *Aeromonas caviae* (the sorbent). This microorganism can in general be found in aquatic environments and consequently in groundwater. As a result, when the experimental data was plotted according to the 2nd order kinetic equation, it was proven that Eq. (1) patently is not appropriate and consequently fails to capture the steep gradient of concentration on the initial stage of removal - see Fig. 2, and the Supplementary material [32].

If the sorption rate is based on uptake by the sorbent, instead of the bulk concentration, it can be described according to the 2nd order equation of Ritchie, from which it can be extracted that one ion of metal occupies two binding sites [33]. It should be noted that in worldwide literature [34], there have been mentions of using a wide range of other kinetic equations, including zero, first (reversible or forward) order, Elovich-type, Langmuir-Hinshelwood, etc.

A suitable description of experimental data, in the case of advancing time, can be provided by equations (2) and (3). It is notable that both kinetic models adequately capture the quick process of adsorption rate during the primary minutes of the experimental studies. However, during the process of biosorption the constant rate of the model of pseudo 2nd order, which is abbreviated as k_m, is monotonously correlated with shifts according to the load of biomass and concentration of bulk [35].

On the contrary, the constant rate, which is derived by the 2nd order equation of Ritchie and is abbreviated as K_2, was found to fluctuate beyond any physical reasoning. Furthermore, better statistical fit can be achieved through Eq. (3). Despite the goodness of the fit at temperatures between 40^o and 60 °C, it was revealed that the reaction rate constant in the case of both models varied randomly, according to the temperature of the process. Using the Arrhenius model for preliminary calculations, which were achieved every time between the two temperatures, always resulted in activation energies lower than 10 kJ/mol, which is far below what was expected for the sorption processes controlled by the reaction. The changes on the morphology of the surface of biomass (sorbent) at different temperatures, and the dependence of capacity of sorption on the value of the temperature may be attributed to the irregularity of surface morphology.

In order to compare various experimental measurements for a study of kinetics, it is mandatory to introduce a degree of conversion with dimensionless form. As a result, with the normalization

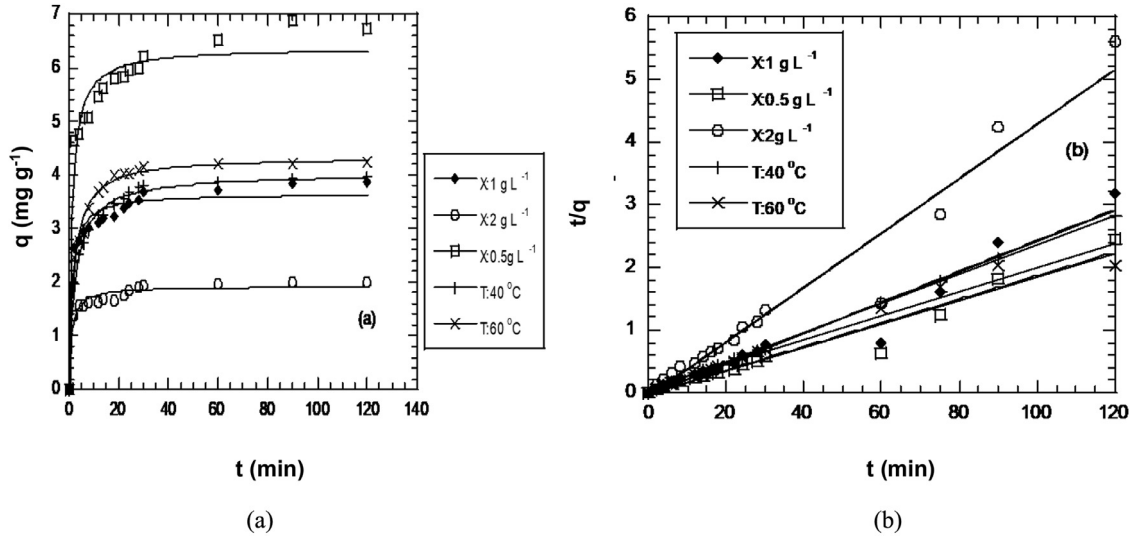

(a) (b)

Fig. 2. Comparison of experimental removal curves (for different temperatures and concentration of biomass) against the predictions of theory based on: (a) 2nd order equation of Ritchie (at 5 mg L-1 initial concentration of cadmium) and (b) pseudo 2nd order equation (at 50 mg L^{-1} initial concentration of cadmium). Reproduced with permission taken by Wiley, 2005 [32].

of the remaining concentration of ions, which is abbreviated as C_t, with accordance to some value of reference, an index of sorption can be determined - i.e., conversion degree (Appendix - Eq. (4)). For the case of intraparticle diffusion, Crank (1975) proposed a model which takes into consideration the uninterrupted reduction of concentration of bulk, due to uptake of sorbate. This phenomenon generates a condition of boundary, which depends on time and relates to the concentration at the sorbent particle surface. The solution of the equation of intraparticle diffusion, Eq. (5), can be solved with a numeral process in order to confirm the constant of effectiveness of time of diffusion, which is abbreviated as ξ. The solution of the equation of intraparticle diffusion has the same expression in the case of a diffusion control of (macro)pore structure, but only when the obtained isotherm of equilibrium has a linear form for the range of concentration, which is under examination. In this article, the experimental study process depends on measuring the residual concentration of metal ions in the bulk, which is abbreviated as Λ, and its value is always above 0.5. When the Λ value is approximately 0.1, the decrease of concentration of bulk becomes significant, and under these circumstances, the hypothesis of a metal concentration with constant values at the sorbent surface will result to an incorrectly high apparent diffusivity. In addition, in order to correlate the concentration that is used in a sorption experiment to a section with linear form, according to the isotherm of equilibrium, the K constant can be restored by the isotherm local slope. As found by the isotherms of experimental study, this can be approximately valid in the case of concentrations that are used in this experimental work. Since our research is mainly focused in the region of short time intervals, at least 200 terms are used in the process of summation, in order to achieve a satisfactory result with high accuracy.

The transfer of external mass has been studied in literature by following a reaction model of pseudo first-order [36]. This analytical method supposes that the concentration of the sorbate on the surface of the sorbent has zero value at all times. Nevertheless, this value is not correct in circumstances where a notable sorbate amount is removed during the adsorption process, with quick rate during the initial stages of the procedure. In addition, a model with a more pragmatic character should instead examine a quick equilibrium phase, being established betwixt the interface and the sorbate, which is presented on the surface of the sorbent [37]; It should also be clarified that this concept is adopted in the present work. Furthermore, if the sorbent surface is combined across the mass balance, the adsorption isotherm of Langmuir method and rate of change in the equation of the bulk concentration can be expressed as equations (8) and (9) after some calculations, which can be converted and solved numerically after further processing. It is notable that with the normalization of C_t^s with assessment to C_o^s - and not C_o as Puranik *et al.* (1999) did - and also the normalization of t with assessment to τ, the solution characteristics are enhanced remarkably. The stability and convergence, which are attributed to the analogous spreading of all variables over the computational domain, are such an example.

Fig. 3a depicts the fitting results from Eq. 5 to the data of sorption which were derived using various initial temperatures, concentrations and solid amounts. In addition, it is apparent that despite that, disperse measurements in the finite volume of the diffusion model can express the entire data range adequately well, involving also the steep gradient of concentration at brief time intervals. This type of behavior is a consequence of decreasing the slope of an equilibrium curve with non-linear form, e.g. in the case of isotherm of Langmuir method, a quickly increase of diffusivity with increasing concentration is generated [38]. Moreover, the performance of kinetic tests for desorption with adsorbent material, which was previously employed for sorption, is a way to further check the possibility of a controlled pore diffusion mechanism. It was hypothesized that at the initial stages of the procedure, the chromium effluent is sorbed via a highly favorable and quite fast mechanism of chemical reaction, such as an ion-exchange, but soon after diffusion of external film comes into play. According to this stage, if the time interval at the primary minute of process of sorption is not taken into consideration, the existing curves fit very favorably the equations (10) & (11) model. These results are revealed in Fig. 3b. Near the end of the sorption process (in the case of a higher value than 0.9), the reaction becomes much slower, e.g., intraparticle diffusion, and becomes gradually the step of rate-controlling. This is a status quo, however, which has no practical significance. In addition, for the assessment of statistical significance of the determination, a derivative analysis of a time series where the d_α/d_t is plotted against the value of t and thereafter has been performed, and a low pass filter is applied by Hanning, in order to flatten out the undulations of signal un-

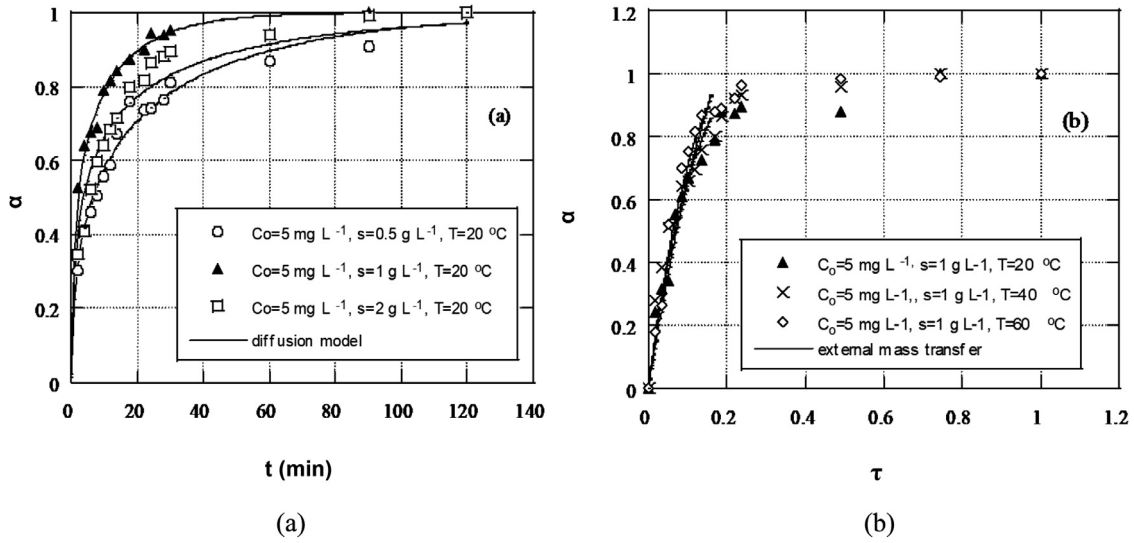

Fig. 3. Experimental degree of conversion, a, at 5 mg L^{-1} initial concentration of chromium against predictions according to the solution of the: (a) equation of diffusion, for various loads of adsorbent and (b) equation of mass transfer, for a wide range of temperatures (where as s is mentioned the load of biomass). Reproduced with permission taken by American Chemical Society, 2004 [40].

til d_α/d_t versus α becomes a reasonable curve with smooth shape [39].

In addition, the α(t), which is the integrated smoothed signal as previously elaborated and lead in values of K_mS that are narrowly comparable to the unfiltered values of experimental data, with no preferential trend in relation to the load of biomass. This is a highly positive additional sign, which confirms that the predominant mechanism may be the external mass transfer of the process of sorption after the initially fast removal of chromium. It is quite common when attempting to achieve high system performance, while at the same time contributes to more than one process. In order to circumvent this problem, a simplifying approach can be used, which supposes that each one of the concurrent procedures dominates over the others (i.e. the step of rate controlling) at specific time intervals of the process, and thereafter studies them independently [41]. Nevertheless the conclusion drawn from the above example suggest that the conducted examination was not appropriate to provide strong evidence in favor of any of the studied mechanisms, since diverse models of kinetics were victorious in the experimental data fitting [42,43].

3. The process

The analysis of kinetics not only allows the estimation of sorption rates, but also results in suitable expressions of rate characteristics and potential reaction mechanisms [44]. A basic thermodynamic investigation of the system usually follows right after. For instance, when the Gibbs free energy has values with negative sign, ΔG^0, the sorption of the examined reactive dye onto layered double hydroxide (the sorbent material) was revealed to be spontaneous, under the conditions of the experimental process, without demanding an induction period [45]. The relatively known equations are presented. The positive values of the standard enthalpy change of sorption ΔH^0 reflects its nature, which, in this case, is endothermic. Additionally, since this adsorption process has an endothermic nature, the quantity that sorbed at the phase of equilibrium grew with temperature rise.

On the other hand, lead ions adsorption on bentonite clay was found to be exothermic and spontaneous [46]. As a result, the adsorption reaction is less favorable in the case of a higher temperature. Other similar studies include the removal of cobalt ions onto activated carbon [17], and modified biochar for antimony sorption [47]. The latter showed an inner-sphere complexation occurring. The above results lead to an in-depth analysis of the real process and revealed its mechanism. A few more examples will be presented below.

The greater performance was attributed to the observed iron oxyhydroxide phase (akaganeite), which can react in the presence of arsenates, since oxy-hydroxides of iron can react in the presence of arsenates as illustrated in Fig. 4. The study of the materials with microporous structure was carried out by N_2 adsorption (BET), SEM, FTIR, thermal analysis and patterns of XRD [48].

Interactions of C_π–cation were mainly attributed to interactions with electrostatic nature between the quadrupole moment of the metallic cation (i.e. lead) and activated carbon aromatic rings [49]. The adsorption of curcumin via metal organic frameworks was affected due to the sites with defective morphology in the framework structure [50]. The sorption of cadmium on biochar was achieved due to the formation of precipitation of $Cd(OH)_2$ and $CdCO_3$ and the interaction with carboxyl and carbonyl groups; whereas in the case of sulphur-modified biochar, the process of sorption was achieved due to the formation of CdS and $CdHS^+$ and to interaction with organic sulphide [51].

4. Examples of sorbents' synthesis

In the experimental study by G. Z. Kyzas et al. [17], activated carbon was synthesized from potato peels according to the following synthetic route: initially, the bio-waste potato peels were leached with deionized water, in order to remove dust and other inorganic compounds. The obtained potato peels were then filtered, in order to remove water and were afterwards oven-dried at 120 °C for a period of 24 h, to rid the content off moisture. The dried bio-waste was ground and sieved, in an attempt to obtain a particle size in the range of 0.45 to 0.15 mm. H_3PO_4 was used as the agent for the activation of dry biomass, through the process of chemical activation. A weighted amount of dried potato peels (10 g) was impregnated with H_3PO_4 (125 mL-75% w/w) at ambient temperature and was kept under stirring for 24 h. Furthermore, the impregnated with H_3PO_4 bio-waste was dried at high temperature in a sand bath, with the purpose to remove residual water and was later oven-dried at a temperature of 100 °C for a 24 h period. In addition, a weighted amount of the dried and impregnated with H_3PO_4 bio-waste samples was inserted in a furnace for

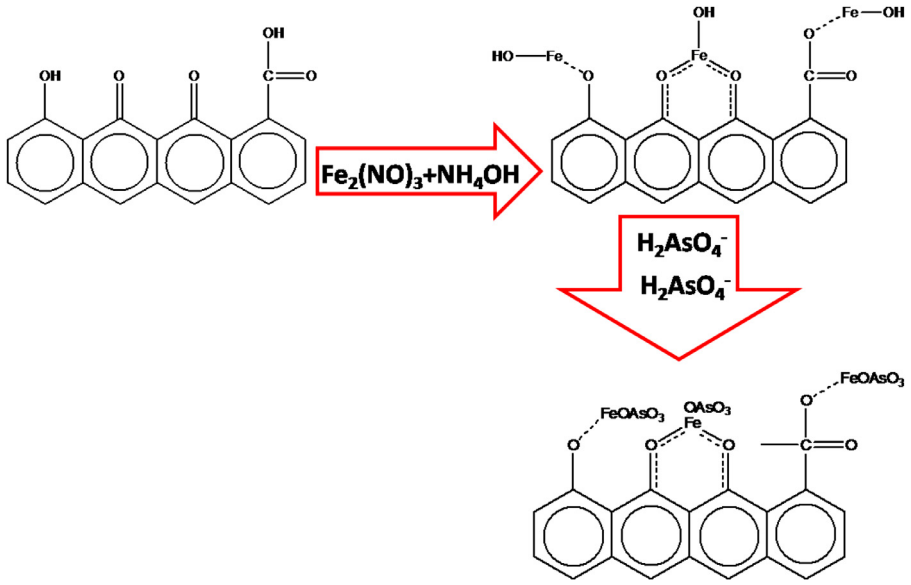

Fig. 4. Arsenates sorbed by iron oxyhydroxide impregnated (microporous) activated carbon: mechanism of the process. Reproduced with permission taken by Bentham Science, 2014 [48].

the process of carbonization and heated up at activation temperatures of 400, 600 and 800 °C under a N_2 flow (99.999% pure) of 30 STP cm^3/min; the latter was kept at the same ratio during the process of heating up and cooling down, keeping the heating rate constant (~10 °C/min). The process of treatment at the temperature of carbonization lasted for a period of 2 h. This was followed by the process of cooling down the residues, which had a solid form and were washed for 24 h in a Soxhlet apparatus, in order to obtain a neutral pH (6-7) value. They were then leached again with the aid of ethanol. Finally, in order to obtain the activated carbon materials, they were dried in an oven for 24 h at a temperature of 100 °C and were abbreviated as PoP400, PoP600 and PoP800 where the ''Po'' term corresponds to the precursor potato peels, "P" to H_3PO_4 activation agent and the numerals "400", "600" and "800" to the temperatures of activation, respectively [17].

In another synthetic protocol from the research activity of G.Z. Kyzas, the synthesis of low-cost adsorbents from untreated coffee residues (UCR) was achieved, which were derived from cafeterias. These coffee residues were used without modification, and thus were untreated. In order to improve their adsorptive ability, the only processing they were submitted to was their leaching in the presence of distilled water, aiming to remove color and dirt, and then they were dried in a convention oven for 5 h at the temperature of 105 °C. The coffee residues that were used for the adsorption studies were in powder form after the process of sieving, reaching a final particle size between 475 and 525 μm [52].

In a different work [53], the synthesis of low-cost adsorbents from "Greek coffee" (COF) was achieved. These coffee residues were used without modification as well, i.e. they were untreated. In order to improve their adsorptive ability, the only processing they were submitted to was their leaching via distilled water in order to remove color and dirt. They were later dried in a convention oven for 5 h at a temperature of 105 °C. The coffee residues that were used for the adsorption studies after the process of sieving were in powder form, with final particle size between 475 and 525 μm [53]. Furthermore, in the same work, the synthesis of low-cost adsorbents was achieved from treated coffee residues (TCR) and UCR. More specifically, in the case of UCR, the residues were dried in just ambient air. Then, the process included the sieving of UCRs in order to obtain particles in the range of 475-525 μm.

In the case of TCR, it was initially washed with distilled water in order to remove color and dirt, and thereafter it was dried in a convection oven for a period time of 5 h at 105 °C. Then, the coffee residues were treated with a 2% solution of formaldehyde, in order to decrease the leaching of organic compounds, and to prevent the formation of mould during batch adsorption. Both, TCR and UCR after the process of sieving were in powder form with final particle size between 475 and 525 μm [54].

Travlou et al. [55] prepared a graphite oxide grafted with magnetic chitosan adsorbent composite. Initially, $FeCl_3$ $6H_2O$ (9.5 g), $FeCl_2$ $6H_2O$ (3.5 g), and then DI water (400 mL) were stirred in a water bath for 1 h at a temperature of 60 °C under a N_2 flow. Thereafter, a solution of ammonia was inserted dropwise, and the mixture was then purged with the use of N_2, until a value of 10 pH was achieved. The obtained precipitation after the aforementioned process was thus decanted in a dialysis tubing membrane, which was manufactured by cellulose material (Sigma Co.). In addition, the cellulose membrane which was filled with the precipitation material was inserted in a bath of distilled water. The membrane was used in order to remove the ions of chloride from the initial suspension, through the osmosis process. The water bath was tested in order to see if there is presence of Cl^- ions. This process was achieved with the use of a 0.1 M solution of $AgNO_3$. Next, the water of the bath was changed and replaced a lot of times in order to achieve after examination the absence of chloride ions in the aqueous solution. After the process of decantation, the cake from the surface of the membrane was obtained and was inserted in a bench freeze drier (Christ Alpha 1-4), where it was freeze-dried [55].

Furthermore, an acetic solution (400 mL-2% v/v) was prepared, where the pure chitosan (Ch_{HMW}, 2 g) was dissolved. Magnetic particles were then inserted in the aforementioned synthesized solution of chitosan (0.75 g), and the prepared mixture was later sonicated for a period of 30 min. In order to achieve the cross-linking of chitosan, the glutaraldehyde solution (GLA, cross-linker) was added to the prepared mixture. The process of cross-linking was carried out because the presence of chitosan in aqueous solution appears to have a high degree of swelling, as well as because the adsorbent nanocomposite that is based on chitosan should be cross-linked in order to overcome this problem. GLA (15 mL, 50 wt. % in H_2O) was inserted in the reaction flask and then the aqueous

solution was stirred vigorously under these conditions for 2 h at the temperature of 60 °C. After this process, the obtained precipitate was rinsed with the aid of ethanol and distilled water. Finally, the obtained material was inserted and dried in a vacuum oven at the temperature of 50 °C. The resulting product obtained after the described process was magnetic chitosan (Chm) [55].

The next step includes the synthesis of GO according to a modified method of Hummers. Commercial powder of graphite (10 g) was stirred in the presence of concentrated H_2SO_4 (230 mL, 0 °C). Thereafter, $KMnO_4$ (30 g) was slowly inserted to the prepared suspension. Because the temperature of the suspension should be kept lower than 20 °C, the addition rate was controlled in order to prevent a quick increase in the suspension temperature. After this process, the reaction mixture was cooled down at the temperature of 2 °C. After the ice bath removal, the obtained mixture was stirred at ambient temperature for 30 min. Distilled water (230 mL) was then added to the reaction vessel at a very slow rate, while the temperature of the reaction was maintained at values lower than 98 °C. The suspension was diluted and further stirred for 15 min and then got diluted again with distilled water (1.4 L); Afterwards, H_2O_2 (100 mL, 30 wt. % in H_2O) was added and it was left overnight. The yielded particles of GO settled at the bottom of the used vial, and were later separated from the excess aqueous solution (liquid) through decantation. The process included the transportation of the remaining suspension to dialysis tubes (Sigma Co.). The process of dialysis was accomplished with the addition of a $BaCl_2$ aqueous solution and precipitation of $BaSO_4$ was not detected. The liquid form of the yielded GO was separated through the process of centrifugation. Finally, the yielded material, which had a gel-like morphology was freeze-dried, and from the initial GO, the final material -a fine dark brown powder- was obtained [55] .

Finally, an acetic solution (100 mL-2% v/v) was prepared, in which the pure chitosan (Ch_{HMW}, 2 g) was dissolved. The synthesized mixture was sonicated for 30 min. In addition, magnetic particles were inserted in the synthesized chitosan solution (0.75 g), and the prepared mixture solution was further stirred for a period of 2 h. GLA was then added to the reaction flask (15 mL, 50 wt. % in H_2O), along with GO (1.5 g). The pH of the mixture was adjusted to 9-10 and thereafter was stirred for 1h at 80 °C. The obtained precipitate was leached with ethanol and distilled water, and finally dried in a vacuum oven at a temperature of 50 °C. The final product, abbreviated as GO-Chm, was grounded in order to obtain its powder form and then sieved in order to reach a final particle size between 75 and 125 μm [55]. Table 1 presents the selected synthetic routes as well as the experimental conditions.

5. Cost analysis

During the initial research stage process, large-scale data was gathered. A top-down approach was adopted in order to estimate and verify the market share of reagents. During the secondary research, information from multiple studies and various sources (industry reports, articles, scientific papers etc.) was taken into account. The reagents market research was conducted through the use of directories and databases, in order to identify and obtain a wide range of data to achieve a more oriented research of the reagents market and related technical processes [56].

5.1. Synthesis cost

The data was collected from various sources, mainly from in-person interviews with Greek Laboratories of Chemistry, due to the personal experience and practice on the subject matter. The main point of the interviews was the identification and assessment of “popular” adsorbents. In-person interviews offer a lot of advantages, such as the observation of the interviewee’s reactions and the unobtrusive listening of their replies. As suggested by Holstein and Gubrium, this work performed interviews of unstructured character, due to their effectiveness and flexibility to explore select issues of great importance. It allows the interviewee to share their personal expertise, without the occasional risk stemming from the guided questions of a researcher. The confidentiality of these interviews is of great importance in order to protect the participants, which enables the free expression of their opinions. In the case of the present work, the interviewees are male professors, while the duration of the interview was more than 40 minutes [56].

5.2. Selection of synthesis route

In order to explore the adsorption phase in more depth and in order to uncover the factors that characterize the adsorption materials, a literature search was conducted with the intention to identify and further examine the selected synthetic routes. In addition, the experimental synthesis routes with the most novelty and citations were selected, in order to evaluate the cost factors [56].

5.3. Cost of raw materials

The cost of raw materials for the study of reagents was retrieved from publicly released catalogues. In the case of chitosan products, there is a wide range of prices which depends on the final product quality. For example, the price of a chitosan product might range between 10 to 1000 USD dollars per kilogram. In this study, the calculated costs are translated to euros (¬).This cost analysis took into account the prices from multiple vendors all over the world. For each case, the cost of raw materials included the cost of the adsorbent and the cost of the recovery materials [57].

5.4. Energy cost

The energy spent during the various stages of the experimental processes corresponds to the cost of energy. The cost of energy per KWh is calculated based on the average energy price in Greece for 2020 (0.197 Euro/KWh), according to the Hellenic Public Power Corporation S.A. As a result, the cost of energy in Euros has been calculated for the amount of KWh spent and the 1 KWh price in Greece.

6. Adsorption applications

6.1. Adsorption Isotherms

In the case of potato peels with activated carbon for the removal of Co (II) ions, the effect of initial concentration of ions on adsorption was calculated according to the isotherms of equilibrium data. Fig. 5 presents this effect at temperature levels of 25, 45 and 65 °C. It should be noted that the adsorption capacity of PoP 400 and PoP 600 increases according to the increase of the initial concentration of Co(II) ions from 10 to 1000 mg/L. After fitting the Freundlich and Langmuir models, it was revealed that the best fitting was achieved with the model of Langmuir when R^2=0.998. Furthermore, it was revealed that the PoP 400 has lower adsorption capacity in comparison to the PoP 600 and the values were 373 and 405 mg/g, respectively, at a temperature of 25°C (Table 2).

This change of 8% is attributed to the difference of structural and textural properties of PoP400 and PoP600 carbons. In addition, the same experiments of equilibrium were also performed at a temperature level of 45 and 65 °C. The behavior of adsorption process was not the same for the PoP400 and PoP600 adsorbents. In

Table 1
Selected syntheses and synthesis conditions.

Materials	Experimental procedure	Instrumentation	Ref.
Activated carbon derived from potato peels *Synthesis materials: H_3PO_4 (125 mL, 75% w/w)*	• Drying (120°C, 24 h)	Oven Thermofisher (1.45 kW)	[17]
	• Sieving (+0.45-0.15 mm, 1 h)	ANALYSETTE 3 PRO (50 W)	
	• Stirring (24 h)	CAT M 6,1 (580 W)	
	• Sand bath (6 h)	Sand bath S70 (1000 W)	
	• Drying (100°C, 24 h)	Oven Thermofisher (1.45 kW)	
	• Activation (2 h)	Oven Thermofisher (1.45 kW)	
	• Nitrogen flow of 30 STP cm^3/min (4 h)	-	
	• Soxhlet (24 h)	Soxhlet Electrothermal (580 W)	
	• Drying (100 °C, 24 h)	Oven Thermofisher (1.45 kW)	
Adsorbent derived from coffee residues *Synthesis materials: Coffee residues*	• Washing (24 h)	CAT M 6,1 (580 W)	[52]
	• Drying (5 h)	Oven Thermofisher (1.45 kW)	
	• Sieving (0.5 h)	ANALYSETTE 3 PRO (50 W)	
	• Washing (24 h)	CAT M 6,1 (580 W)	[53]
	• Drying (5 h)	Oven Thermofisher (1.45 kW)	
	• Sieving (0.5 h)	ANALYSETTE 3 PRO (50 W)	
	• Washing (24 h)	CAT M 6,1 (580 W)	[54]
	• Stirring with formaldehyde (12 h)	CAT M 6,1 (580 W)	
	• Drying (5 h)	Oven Thermofisher (1,45 kW)	
	• Sieving (0.5 h)	ANALYSETTE 3 PRO (50 W)	
Magnetic nanoparticles *Synthesis materials:* Acetone (200 mL), $FeCl_2 \bullet 4H_2O$ (3.5 g), $FeCl_3 \bullet 6H_2O$ (9.5 g), doubly distilled water (400 mL), ammonia (50 mL), N_2 flow 150 cm^3/min, $AgNO_3$ (0.5 g), distilled water (2 L)	• Washing (24 h)	Soxhlet Electrothermal (580 W)	[55]
	• Stirring (1 h)	CAT M 6,1 (580 W)	
	• Water bath (1 h)	Precision GP 02 (200 W)	
	• Dialysis tubing cellulose membrane (24 h)	-	
Magnetic chitosan *Synthesis materials:* Pure chitosan (Ch_{HMW}, 2 g), acetic acid solution (400 mL, 2% v/v),magnetic particles (0.75 g), GLA (15 mL,(50 wt% in water)), ethanol (500 mL), distilled water (500 mL)	• Stirring for the dissolving of chitosan in acetic acid (1 h)	CAT M 6,1 (580 W)	[55]
	• Sonication (0.5 h)	Sonicator Fisherbrand (500 W)	
	• Cross-linking (12 h)	CAT M 6,1 (580 W)	
	• Vigorous stirring (2 h)	CAT M 6,1 (580 W)	
	• Vacuum oven (12 h)	Oven Thermofisher (1.45 kW)	
Graphite oxide *Synthesis materials:* Graphite powder (10 g), H_2SO_4 (230 mL), $KMnO_4$ (30 g), distilled water (1.63 L), H_2O_2 (100 mL, 30 wt% in H_2O), $BaCl_2$	• Time of process ($KMnO_4$ addition)-stirring under ice bath (after ice bath +30 min further stirring) (2 h)	CAT M 6,1 (580 W)	[55]
	• Centrifugation (1 h)	Sorvall ST 8 Small Benchtop Centrifuge (310 W)	
	• Freeze-drying (12 h)	Christ Alpha 1-4 (510 W)	
Graphite oxide-magnetic chitosan composite *Synthesis materials:* Pure chitosan (Ch_{HMW}, 2 g), acetic acid solution (100 mL, 2% v/v (%vol)), Magnetic particles (0.75 g), GLA (15 mL,(50 wt% in H_2O)), GO (1.5 g), ethanol 500 mL, distilled water (2 L)	• Sonication (0.5 h)	Sonicator Fisherbrand (500 W)	[55]
	• Stirring (3 h)	CAT M 6,1 (580 W)	
	• Vacuum oven (12 h)	Oven Thermofisher (1.45 kW)	
	• Sieving (1 h)	ANALYSETTE 3 PRO (50 W)	

the case of PoP400, the adsorption capacity (Q_{max}) increased from 373 mg/g to 382 and 389 mg/g for adsorption temperature levels of 25, 45 and 65 °C, respectively (Table 3). The percentage increase of Q_{max} was 2.4 % after increasing the temperature from 25 to 45 °C, and 1.8 % after moving from 45 to 65 °C. However, in the case of PoP600 the increase of temperature seems to have a greater influence. In the case of PoP600, the Q_{max} increased from 405 mg/g to 447 and 480 mg/g for adsorption temperature levels of 25, 45 and 65 °C, respectively (Table 3). The percentage increase of Q_{max} was 10.4 % after going from 25 to 45 °C, and 7.4 %, when increasing from 45 to 65 °C. Finally, after a comparison of the PoP400 and PoP600 carbons, it was revealed that in the case of PoP600 the influence of temperature was about 5-8 times higher than PoP400 [17].

In the case of UCR for the removal of dyes from aqueous solution, the data of experiments were fitted to the isotherm models of Langmuir, Freundlich and Langmuir-Freundlich (L-F), respectively. Fig. 6 presents the obtained isotherms which were derived from the adsorption of Remazol Blue RN and Basic Blue 3G onto UCR. The results of Q_{max} (Table 2), are presented below along with the other equilibrium parameters which were derived after the process of experimental data fitting (Table 3). The correlation coefficients (R^2>0.997) reveal that the results derived from the model of L-F appear to have a better fitting and a closer prediction. In addition, the calculated Q_{max} at the temperature of 25 °C for Remazol Blue RN and Basic Blue 3G were 179 and 295 mg/g, respectively (Table. 2).

The equilibrium uptake of dye for all cases of adsorbents was affected by the initial concentration of dye, using constant adsorbent dosage (1 g/L). In the case where the initial concentrations are low, the equilibrium phase is reached very rapidly because the dyes' adsorption (basic or reactive) is very intense. This result indicates the possible formation of dye molecules monolayer coverage at the outer interface of UCR adsorbent. Moreover, in the case of low concentrations (0-50 mg/L), the initial ratio of the number of dye molecules to the accessible sites of adsorption is low, and later on becomes independent. Therefore, according to Brunauer et al. the curves shapes of Fig. 6 indicate that the obtained isotherms

Table 2
Selected synthetic routes for the removal of various pollutants by using different adsorbents (dosage: 1 g of adsorbent per 1 L of adsorbate solution at 25 °C).

Material produced	pH	Q_{max} (mg/g)	Pollutant	Ref.
Activated carbon from potato peels (PoP 400)	6	373	Co(II)	[17]
Activated carbon from potato peels (PoP 600)	6	405	Co(II)	[17]
Adsorbent derived from coffee residues UCR	2	179	Remazol Blue RN	[52]
	10	295	Basic Blue 3G	[52]
	2	241	Reactive dyes	[53]
	8	5	Cu(II)	[54]
	8	44	Cr (VI)	[54]
Adsorbent derived from coffee residues TCR	8	69	Cu(II)	[54]
	8	37	Cr(VI)	[54]
Graphene oxide and magnetic chitosan	3	391	Reactive Black 5	[55]

Table 3
Equilibrium parameters for the adsorption of various pollutants from aqueous solution with the use of various adsorbent materials.

Langmuir equation				Freundlich equation			L-F equation					Pollutant	Ref.
T (°C)	Q_{max} (mg/g)	K_L (L/mg)	R^2	K_F ($mg^{1-1/n}L^{1/n}$ g^{-1})	n	R^2	Q_{max} (mg/g)	K_{LF} ((L/mg) $^{1/b}$)	b	R^2			
Activated carbon derived from potato peels (PoP400)													
25	373	0.035	0.998	57.68	3.31	0.937	-					Co(II)	[17]
45	382	0.041	0.998	63.55	3.42	0.936	-	-	-	-			[17]
65	389	0.047	0.997	69.52	3.53	0.934	-	-	-	-			[17]
Activated carbon derived from potato peels (PoP600)													
25	405	0.050	0.995	72.40	3.50	0.947	-	-	-	-		Co(II)	[17]
45	447	0.057	0.988	82.27	3.49	0.959	-	-	-	-			[17]
65	480	0.076	0.982	95.64	3.57	0.966	-	-	-	-			[17]
Adsorbent derived from coffee residues													
25	175	0.009	0.997	11.84	2.53	0.956	179	0.008	0.96	0.997		Remazol Blue RN	[52]
45	197	0.008	0.998	11.83	2.53	0.957	212	0.007	0.90	0.999			[52]
65	232	0.007	0.997	11.44	2.27	0.980	269	0.005	0.83	0.999			[52]
25	240	0.041	0.987	36.61	3.12	0.974	295	0.020	0.67	0.998		Basic Blue 3G	[52]
45	245	0.044	0.984	38.33	3.15	0.978	313	0.018	0.64	0.999			[52]
65	251	0.048	0.978	41.44	3.21	0.982	347	0.014	0.58	0.999			[52]
25	214	0.0075	0.997	11.47	2.34	0.976	241	0.0054	0.850	0.999		Reactive dyes	[53]
45	245	0.0072	0.997	12.08	2.27	0.978	278	0.0051	0.848	0.999			[53]
65	254	0.0091	0.997	15.85	2.43	0.975	287	0.0064	0.835	0.999			[53]
25	49.34	0.222	0.978	16.842	4.02	0.964	59.18	0.132	0.64	0.996		Cu(II)	[54]
25	56.90	0.229	0.973	19.245	3.94	0.924	69.97	0.125	0.61	0.993			[54]
25	38.68	0.139	0.995	11.739	3.90	0.915	37.03	0.150	1.18	0.998		Cr(VI)	[54]
25	43.75	0.136	0.996	12.505	3.67	0.940	44.82	0.129	0.93	0.996			[54]
Graphene oxide with magnetic chitosan (GO-Chm)													
25	368	0.113	0.944	39.99	2.18	0.991	391	0.148	0.60	0.954		Reactive Black 5	[55]
45	372	0.067	0.969	59.21	2.56	0.996	401	0.056	0.81	0.970			[55]
65	391	0.037	0.976	93.48	3.27	0.989	425	0.030	0.85	0.964			[55]

for the studied system of adsorbent-dye are Type-I, according to the classification of BET, and are characterized by a high adsorption degree at low concentrations. In the case of higher concentrations, the availability of sites of adsorption become lower and subsequently the process of adsorption depends on the initial dye concentration. In fact, the exchanging molecules and their diffusion within the particles of UCR, may govern the rate of adsorption in the case of higher initial concentrations. The temperature effect on the phase of equilibrium is presented via the curves of isotherm (Fig. 6). The behavior of adsorption is the same for Remazol Blue RN and Basic Blue 3G: after an increase of the procedure's temperature from 25 to 65 °C, an increase of the Q_{max} (dye uptake) is observed. However, the adsorption increase is mainly attributed to the augmentation of the adsorption sites number, which is caused due to the breaking of some of the internal bonds near the edge of the active sites of surface of the UCR adsorbent. Likewise, the phenomenon of the adsorption increase could be attributed to the increased dye molecules penetration inside the possible structure of micropores or apparent cavities on surface in the case of higher temperatures or to the new active sites creation [52].

Fig. 7 depicts the isotherms which were obtained from the synthetic effluent decolorization at two values of pH (in order to compare the obtained Q_{max} of COF at optimum and natural value of pH). Moreover, below are reported the maximum Q_{max} and the other parameters of isotherm which were obtained after the fitting process (Table 3). The correlation coefficients (R^2) confirmed that the models of Langmuir and L-F fit with high correlation to the experimental data (Langmuir: R^2 ~ 0.997; L-F: R^2 ~ 0.999). In the case of total dye removal at 25 °C the Q_{max} was 179 mg/g (pH = 10) and 241 mg/g (pH = 2). Furthermore, it should be noted that the current study describes the COF application not only for synthetic samples, but and for real dyeing samples. In general, it was observed that the equilibrium uptake of dye was affected by the initial concentration of dye, using constant COF dosage (1 g/L). In the case of low initial concentrations, the equilibrium phase was

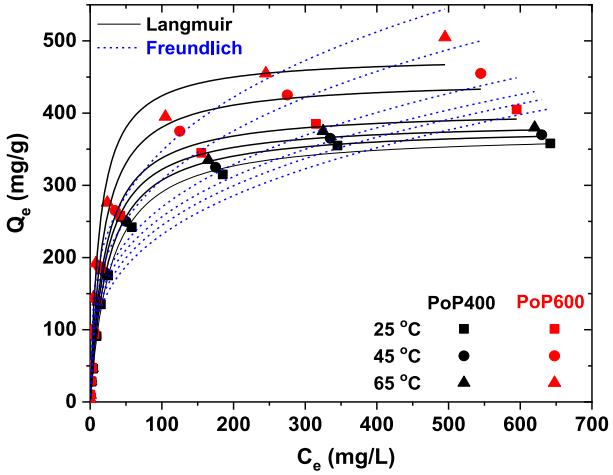

Fig. 5. Effect of temperature (25, 45, 65 °C) and initial concentration on adsorption of Co (II) chemical element onto PoP600 and PoP400 (fitting to isotherm equations of Freundlich and Langmuir). Reproduced with permission taken by Elsevier, 2016 [17].

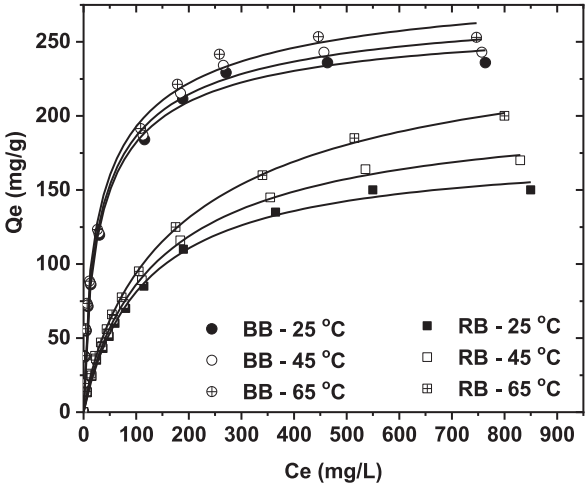

Fig. 6. Effect of temperature and initial concentration of dye (isotherms) on adsorption of Basic Blue 3G and Remazol Brilliant Blue RN onto untreated coffee residues (pH = 10, Basic Blue 3G; pH = 2, Remazol Brilliant Blue RN; concentration of dye 0-1000 mg L^{-1}; 24 h contact; 140 rpm; 1 g L^{-1} adsorbent; T = 25, 45, 65 °C). Reproduced with permission taken by Elsevier, 2012 [52].

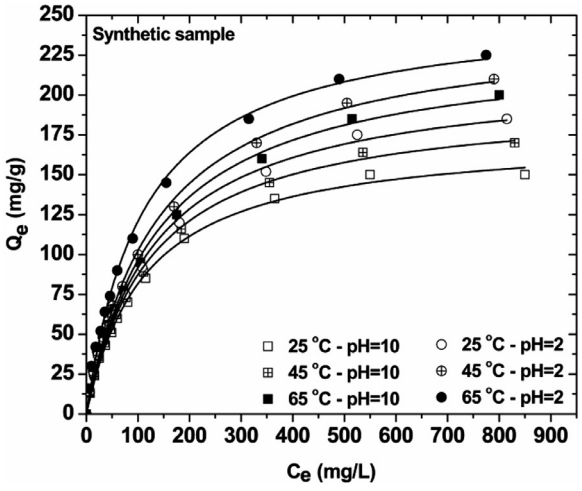

Fig. 7. Decolorization isotherms of synthetic solution dyeing with Greek coffee grounds (pH = 2, 10; total concentration of dye 0-1000 mg L^{-1}; 24 h contact, 140 rpm, 1 g L^{-1} adsorbent, T = 25, 45, 65 °C). Reproduced with permission taken by MDPI AG, 2012 [53].

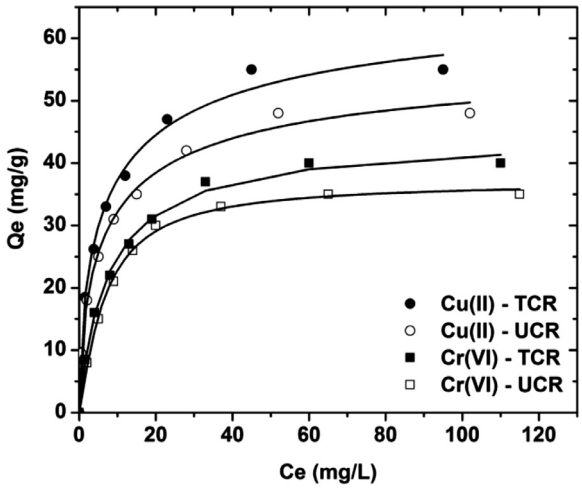

Fig. 8. Effect of initial concentration of ion on removal of Cr (VI) and Cu (II) onto treated and untreated residues of coffee (pH = 5; concentration of ion 0-50 mg L^{-1}; 5 min - 24 h contact; 140 rpm; 1 g L^{-1} adsorbent; T = 25 °C). Reproduced with permission taken by MDPI AG,2012 [54].

reached very rapidly because the dyes adsorption was very intense. In conclusion, this phenomenon confirms the possibility of monolayer coverage formation of molecules of dye at the outer COF interface.

In the case of low total concentrations of dye (0-50 mg/L), the initial ratio of dye molecules to the available sites of adsorption is low, and the fractional adsorption has independent character according to the initial concentration. As a result, according to Brunauer et al., the curve shapes of Fig. 7 indicate that the obtained isotherms for the studied system of adsorbent-dye are Type-I, according to the classification of BET, and are characterized by a high adsorption degree at low concentrations. Furthermore, in the case of higher concentrations, the available sites of adsorption were lower and the process of adsorption depended on the initial dye concentration. In fact, the exchanging molecules and their diffusion within the particles of COF, may govern the adsorption rate in the case of higher initial concentrations. The temperature effect on the phase of equilibrium is presented via the curves of isotherm (Fig. 7). The behavior of adsorption is the same for both conditions of pH of synthetic effluents: when increasing the procedure's temperature level from 25 to 65 °C, an increase of the Q_{max} was observed (dye uptake) [53].

The fitting parameters of the three isotherm models are presented in Table 3. The correlation coefficient values (R^2~0.998) confirm that the model of L-F appears to have a better fit and the closest prediction. The initial metal concentration effect on the adsorption metal loading of the coffee residues is depicted in Fig. 8. The obtained data suggested an increase in the metal's amount, which adsorbed onto the adsorbents derived from coffee residues, when the initial concentration of metal was increased. It was observed that the Q_{max} change between the TCR and UCR was approximately 10 mg/g. (Cr(VI): 44 mg/g, TCR; 37 mg/g, UCR and Cu(II) 69 mg/g, TCR; 5 mg/g, UCR) [54].

Fig. 9 depicts the isotherm curves of GO and GO-Chm. The parameters of the fitting of the three isotherm models are presented in Table 3. For the Reactive Black 5 removal, the Q_{max} at 25 °C was 391 mg/g (Table 2). The equilibrium uptake of dye for all cases of adsorbents was affected by the initial concentration of dye using constant adsorbent dosage (1 g/L). When the initial concentrations are low, the equilibrium phase is reached very rapidly because the dye's adsorption (basic or reactive) is very intense. This result indicates the possible formation of dye molecules monolayer coverage

Table 4
Comparison of the pseudo first-second and third-order adsorption rate constants.

Adsorbent	Pseudo-first order		Pseudo-second order		Pseudo-third order		Pollutant	Ref
	k_1 (min^{-1})	R^2 (-)	k_2 (min^{-1})	R^2 (-)	k_3 (min^{-1})	R^2 (-)		
Activated carbon derived from potato peels (PoP400)	0.0272	0.997	0.0479	0.955	-	-	Co(II)	[17]
Activated carbon derived from potato peels (PoP600)	0.0344	0.997	0.0607	0.952	-	-	Co(II)	[17]
Adsorbent derived from coffee residues UCR	0.039	0.953	0.071	0.992	0.155	0.941	Remazol Blue RN	[52]
Adsorbent derived from coffee residues UCR	0.065	0.985	0.120	0.994	0.324	0.891	Basic Blue 3G	[52]
Adsorbent derived from coffee residues UCR-Real effluent	0.013	0.994	0.026	0.967	0.051	0.889	Reactive dyes	[53]
Adsorbent derived from coffee residues UCR-Synthetic effluent	0.021	0.994	0.031	0.966	0.058	0.877	Reactive dyes	[53]
Adsorbent derived from coffee residues UCR	0.032	0.998	0.061	0.963	0.128	0.872	Cu(II)	[54]
Adsorbent derived from coffee residues TCR	0.037	0.995	0.070	0.972	0.153	0.887		[54]
Adsorbent derived from coffee residues UCR	0.025	0.994	0.046	0.973	0.093	0.889	Cr(VI)	[54]
Adsorbent derived from coffee residues TCR	0.032	0.998	0.061	0.966	0.127	0.876		[54]
Graphene oxide with magnetic chitosan (GO-Chm)	1.94	0.847	3.255	0.972	-	-	Reactive Black 5	[55]

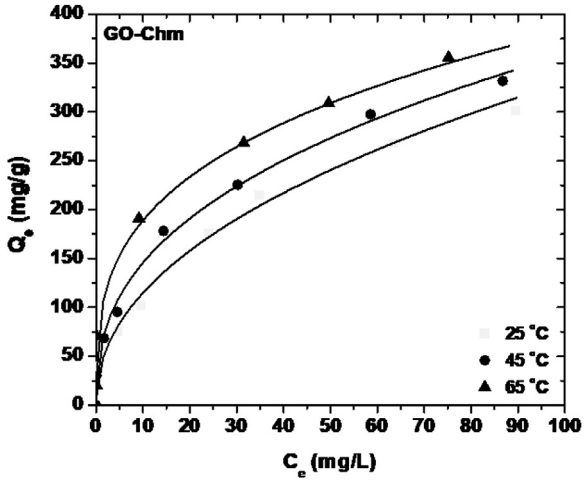

Fig. 9. Effect of initial concentration of Remazol Black 5 on adsoprtion onto GO-Chm. Reproduced with permission taken by American Chemical Society, 2013 [55]

at the outer interface of the GO-Chm adsorbent. Moreover, in the case of low concentrations (0-50 mg/L), the initial ratio number of dye molecules to the accessible sites of adsorption is low, and becomes independent and the fractional adsorption on initial concentration. The temperature effect on the phase of equilibrium is presented via the curves of isotherm (Fig. 9).

It was also revealed that when the procedure's temperature increases from 25 to 65 °C, an increase of the Q_{max} (dye uptake) value is noted. In the case of GO-Chm composite material, the Q_{max} value was increased from 391 mg/g at 25 °C to 401 and 425 mg/g at 45 and 65 °C, respectively. The adsorption increase is however mainly attributed to the augmentation of the adsorption sites number, which is caused due to breaking of the internal bonds near the edge of the active sites of the surface of the UCR adsorbent. Likewise, the phenomenon of increase of adsorption could be attributed to the increased dye molecules penetration inside the possible structure of micropores or apparent cavities on surface, in the case of higher temperatures, or to the new active sites creation [55]. Table 4 presents a comparison of the pseudo-first, -second and –third order adsorption rate constants for all samples.

6.2. Cost calculations

In order to calculate the costs of the selected synthetic routes, Table 1 was designed, revealing all the synthesis information. The methods and duration used during the process of synthesis are presented, along with the appropriate instrumentation (apparatus) and the consumption of energy information. In addition, Table 5 summarizes the costs calculated from the use of raw materials and energy, while the sums of costs of selected synthetic routes are also revealed. The synthetic routes costs will be the basis for the final comparison of the costs for each one of the synthesized adsorbents in this study. The equation that was used for the calculation of the energy cost is presented below:

$$E_c = P_d \times a \times t \times C_c \quad (1)$$

where E_c, P_d, a, t, and C_c refer to the cost of energy (¬), the device power consumption (kW), the load factor (a = 0.5 if the device was used in half-power mode, while in full mode a = 1), the time period that the device (h) is used and the cost of energy (¬/kWh), respectively [57].

6.4. Comparisons with recent literature

The results of this work should be compared to some recently published adsorbent materials in order to evaluate their feasibility. A very high adsorption capacity of 405 mg/g [58] was observed for the case of activated carbon derived from potato peel for the removal of Co(II) from aqueous solution. In the study of Zhang et al., the adsorption of Co(II) from aqueous solution using a layered metal sulfide adsorbent was examined, and its adsorption capacity was found to be 82 mg/g. In another study, the removal of Co(II) from aqueous solution using graphene oxide was examined, resulting in a adsorption capacity of 53 mg/g [59]. Table 6 presents a more detailed comparative study for the adsorption of heavy metals and dyes from aqueous solutions. In the synthetic route of Khalifa et. al. the removal of Cu(II) from aqueous solutions with the use of Cellulose-g-poly(acrylonitrile) was investigated (the adsorption capacity was 13 mg/g), while in another study daily manure biochar was used as adsorbent and the adsorption capacity of Cu(II) removal was found to be 54 mg/g [60]. Kyzas et al. studied the removal of Cu(II) from aqueous solution with treated coffee residues presenting efficient capacity (69 mg/g) [54]. In the study of Mikhaylov et al., the removal of Cr(VI) from aqueous solution using γ-AlOOH/α-Fe_2O_3 composite powders was examined [61], while in another study from Jianhua Q. et al. the removal of Cr(VI) from aqueous solution using KOH-activated porous biochar was examined and the adsorption capacity was found to be 117 mg/g [62]. It is important to note that it is difficult to obtain a direct comparison of adsorbent materials especially for heavy metals and dye compounds. Each material presented in Table 6 has its own properties, disadvantages (adsorption properties, synthesis cost etc.) or advantages (surface characteristics etc.). Furthermore, another important factor that may affect the adsorption capacity of the adsorbate material is the different molecular weights of the absorbance compounds.

Table 5
Costs of raw materials and energy in selected synthetic routes.

Material produced	Raw materials (characteristics)	Raw materials cost (¬)	Energy (¬)	Final price (¬)	Ref.
Activated carbon derived from potato peels	Potato peels bio-waste (free of moisture and sieved), H_3PO_4 (85 wt% in H_2O)	H_3PO_4 (8.35 €)	13.91	22.26	[17]
Adsorbent derived from coffee residues UCR	Coffee residues (free of moisture and sieved)	Distilled water (0.10 €)	2.10	2.20	[52-54]
Adsorbent derived from coffee residues TCR	Coffee residues (free of moisture and sieving after the treatment with formaldehyde); formaldehyde	Distilled water (0.10 €); Formaldehyde (2 €)	2.78	4.98	[54]
Magnetic chitosan and graphene oxide	Acetone; $FeCl_2 \bullet 4H_2O$ (p.a>99.0%), $FeCl_3 \bullet 6H_2O$ (reagent grade, 97%), doubly distilled water, ammonia, $AgNO_3$, distilled water, N_2 flow, Pure chitosan (High molecular weight), acetic acid (> 99%), GLA (50 wt% in water), ethanol, acetone, graphite powder, H_2SO_4 (95%-98%), $KMnO_4$ (>99%), H_2O_2 (30 wt% in water), $BaCl_2$	Acetone (11.2 €), $FeCl_2 \bullet 4H_2O$ (0.52 €), $FeCl_3 \bullet 6H_2O$ (1.92 €), doubly distilled water (0.16 €), ammonia (0.32 €), $AgNO_3$ (1.43 €), distilled water (1.03 €), N2 flow (0.53 €), Pure chitosan (3.64 €), acetic acid (3.55 €), GLA (2.48 €), ethanol (19.66 €), acetone (28.2 €), graphite powder (0.16 €), H_2SO_4 (11.04 €), $KMnO_4$ (4.17 €), H_2O_2 (12.72 €)	6.70	109.43	[55]

Table 6
Comparison of adsorption capacity value between the synthesized materials and other adsorbents. The table has selected metal ions and dyes

Pollutant	Adsorbent	Q_{max} (mg/g)	Ref
Cu(II)	TCR	69	[54]
	Cellulose-g-poly(acrylonitrile)	13	[60]
	Daily manure biochar	54	[60]
Cr(VI)	UCR	44	[54]
	Orange peels	7	[63]
	γ-AlOOH/α-Fe_2O_3 composite powders	4.17	[61]
	KOH - activated porous biochar	117	[62]
Co(II)	PoP 600	405	[17]
	Geopolymer/faujasite	134	[60]
	Chitosan functionalized with thiourea groups	83	[64]
	Activated carbon cloth/graphene oxide electrode	17	[60]
	Magnetic cyanoethyl chitosan beads	28	[60]
	Activated carbon (*Citrus limetta* leaves)	61	[65]
Remazol Blue RN	UCR	179	[52]
	Organobentonites	40	[66]
	Bone char	21	[67]
	Organophilic bentonites	163-287	[68]
Basic Blue 3G	UCR	290	[52]
Basic Blue 66	Cationic starch intercalated montmorillonite	50	[69]
Methylene Blue	Apple pomace	108	[70]
	Fe-Mn binary oxide nanoparticles	72	[70]
	Raw KT3B kaolin (Algeria)	53	[70]
Reactive Black 5	Graphene oxide and magnetic chitosan	368	[55]
	Carbon nanotubes	15	[71]
	Chitosan/quartzite composite	171	[72]
	3-D graphene-based composite	639	[73]
	Coffee residues	78	[74]

7. Conclusions

This review paper investigates the modern trends of sorption, presenting examples of the use of sorbents for the removal of dyes and heavy metal ions, in line with estimations of the cost fingerprint through combined calculations of raw material and energy data. According to the comparison to the results of research works discussed above, it can be concluded that coffee residues can be used as effective adsorbents for the removal of dyes and heavy metal ions from aqueous solutions, at practically zero-cost. These coffee-adsorbents appear to have high adsorption capacity and reusability for more than 10 cycles versus both pollutants. In the case of Basic Blue 3G and Remazol Blue RN removal from an aqueous solution with untreated coffee residues, removal of 51% and 86%, respectively were observed. The high adsorption capacity and reusability deem coffee residues a hot research topic, especially for the removal of dyes from aqueous solutions. In addition, the activated carbon derived from potato peels appears to have extremely high adsorption capacity, when compared to other studies, for the removal of cobalt ions from aqueous solution. The percentage removal of cobalt ions from aqueous solutions reaches 92%, which combined with its high adsorption capacity (405 mg/g) render this type of activated carbon a very effective adsorbent for the removal of cobalt ions from aqueous solutions. The low cost of adsorbents (including graphene with magnetic chitosan) automatically marks these cost-effective adsorbents as very promising adsorbent materials for the removal of dyes and heavy metals from aqueous solutions, while also addressing environmental concerns.

Declaration of Competing Interest

On behalf of all authors, the corresponding author states that there is no conflict of interest. Also, The authors declare that they have no known competing financial interests or personal relationships that could have appeared to influence the work reported in this paper.

CRediT authorship contribution statement

Efstathios V. Liakos: Investigation, Methodology, Writing - original draft, Writing - review & editing. **Despina A. Gkika:** Investigation, Methodology, Writing - original draft, Writing - review & editing. **Athanasios C. Mitropoulos:** Investigation, Methodology, Writing - original draft, Writing - review & editing. **Kostas A. Matis:** Investigation, Methodology, Writing - original draft, Writing - review & editing. **George Z. Kyzas:** Investigation, Methodology, Writing - original draft, Writing - review & editing, Supervision.

Acknowledgements

The financial support received for this study from the Greek Ministry of Development and Investments (General Secretariat for Research and Technology) through the research project "Development of NAnotechnology-enabled "next-generation" Membranes and their applications in Low-Energy, zero liquid discharge Desalination membrane systems"/NAMED (Grant no: T2ΔΓΕ-0597) and it is gratefully acknowledged. Also, many thanks to Profs. T.D. Karapantsios and E.A. Deliyanni (Department of Chemistry, Aristotle University of Thessaloniki, Greece) for their invaluable help and guidance.

References

[1] A. Si, K. Pal, S. Kralj, G.S. El-Sayyad, F.G. de Souza, T. Narayanan, Sustainable preparation of gold nanoparticles via green chemistry approach for biogenic applications, Materials Today Chemistry (2020) 17.
[2] G.Z. Kyzas, M. Kostoglou, Green adsorbents for wastewaters: A critical review, Materials 7 (1) (2014) 333–364.
[3] M. Gaidi, K. Daoudi, S. Columbus, A. Hajjaji, M.A.E. Khakani, B. Bessais, Enhanced photocatalytic activities of silicon nanowires/graphene oxide nanocomposite: Effect of etching parameters, Journal of Environmental Sciences (China) 101 (2021) 123–134.
[4] S. Abd El-Nasser, S. Kim, H. Yoon, R. Toth, K. Pal, M. Bechelany, Sodium-assisted TiO2 nanotube arrays of novel electrodes for photochemical sensing platform, Organic Electronics 76 (2020) 105443.
[5] K. Dua, R. Wadhwa, G. Singhvi, V. Rapalli, S.D. Shukla, M.D. Shastri, G. Gupta, S. Satija, M. Mehta, N. Khurana, R. Awasthi, P.K. Maurya, L. Thangavelu, S. Rajeshkumar, M.M. Tambuwala, T. Collet, P.M. Hansbro, D.K. Chellappan, The potential of siRNA based drug delivery in respiratory disorders: Recent advances and progress, Drug Development Research 80 (6) (2019) 714–730.
[6] N. Dwivedi, J. Shah, V. Mishra, M. Tambuwala, P. Kesharwani, Nanoneuromedicine for management of neurodegenerative disorder, Journal of Drug Delivery Science and Technology 49 (2019) 477–490.
[7] Fitzpatrick, S. F. Prolyl hydroxylase-1 regulates hepatocyte apoptosis in an NF-kBdependent manner. https://pubmed.ncbi.nlm.nih.gov/27130823/
[8] A.A.A. Aljabali, H.A. Bakshi, F.L. Hakkim, Y.A. Haggag, K.M. Albatanyeh, Al Zoubi, M. S., B. Al-Trad, M.M. Nasef, S. Satija, M. Mehta, K. Pabreja, V. Mishra, M. Khan, S. Abobaker, I.M. Azzouz, H. Dureja, R.M. Pabari, A.A.K. Dardouri, P. Kesharwani, G. Gupta, S.D. Shukla, P. Prasher, N.B. Charbe, P. Negi, D.N. Kapoor, D.K. Chellappan, M.W. da Silva, P. Thompson, K. Dua, P. McCarron, M.M. Tambuwala, Albumin nano-encapsulation of piceatannol enhances its anticancer potential in colon cancer via downregulation of nuclear p65 and HIF-1α, Cancers 12 (1) (2020).
[9] T. Zaheer, K. Pal, I. Zaheer, Topical review on nano-vaccinology: Biochemical promises and key challenges, Process Biochemistry 100 (2021) 237–244.
[10] K. Pal, A.A. Aljabali, S. Kralj, S. Thomas, F. Gomes de Souza, Graphene-assembly liquid crystalline and nanopolymer hybridization: A review on switchable device implementations, Chemosphere (2021) 263.
[11] K. Pal, A. Si, G.S. El-Sayyad, M.A. Elkodous, R. Kumar, A.I. El-Batal, S. Kralj, S. Thomas, Cutting edge development on graphene derivatives modified by liquid crystal and CdS/TiO<inf>2</inf>hybrid matrix: optoelectronics and biotechnological aspects, Critical Reviews in Solid State and Materials Sciences (2020).
[12] H. Bensalah, S.A. Younssi, M. Ouammou, A. Gurlo, M.F. Bekheet, Azo dye adsorption on an industrial waste-transformed hydroxyapatite adsorbent: Kinetics, isotherms, mechanism and regeneration studies, Journal of Environmental Chemical Engineering 8 (3) (2020).
[13] G.Z. Kyzas, E.A. Deliyanni, K.A. Matis, Graphene oxide and its application as an adsorbent for wastewater treatment, Journal of Chemical Technology and Biotechnology 89 (2) (2014) 196–205.
[14] L. Yi, L. Zuo, C. Wei, H. Fu, X. Qu, S. Zheng, Z. Xu, Y. Guo, H. Li, D. Zhu, Enhanced adsorption of bisphenol A, tylosin, and tetracycline from aqueous solution to nitrogen-doped multiwall carbon nanotubes via cation-π and π-π electron-donor-acceptor (EDA) interactions, Science of The Total Environment (2020) 719.
[15] G. Chen, C. Wang, J. Tian, J. Liu, Q. Ma, B. Liu, X. Li, Investigation on cadmium ions removal from water by different raw materials-derived biochars, Journal of Water Process Engineering (2020) 35.
[16] P. Prasher, M. Sharma, H. Mudila, G. Gupta, A.K. Sharma, D. Kumar, H.A. Bakshi, P. Negi, D.N. Kapoor, D.K. Chellappan, M.M. Tambuwala, K. Dua, Emerging trends in clinical implications of bio-conjugated silver nanoparticles in drug delivery, Colloids and Interface Science Communications (2020) 35.
[17] G.Z. Kyzas, E.A. Deliyanni, K.A. Matis, Activated carbons produced by pyrolysis of waste potato peels: Cobaltions removal by adsorption, Colloids and Surfaces A: Physicochemical and Engineering Aspects 490 (2016) 74–83.
[18] Z. Aksu, Equilibrium and kinetic modelling of cadmium(II) biosorption by C. vulgaris in a batch system: effect of temperature, Separation and Purification Technology 21 (3) (2001) 285–294.
[19] A.I. Zouboulis, K.A. Matis, I.C. Hancock, Biosorption of metals from dilute aqueous solutions, Separation and Purification Methods 26 (2) (1997) 255–295.
[20] E. Deliyanni, T. Bandosz, K. Matis, Impregnation of activated carbon by iron oxyhydroxide and its effect on arsenate removal, Journal of Chemical Technology and Biotechnology (2013) 88.
[21] A. Esposito, F. Pagnanelli, A. Lodi, C. Solisio, F. Vegliò, Biosorption of heavy metals by Sphaerotilus natans: An equilibrium study at different pH and biomass concentrations, Hydrometallurgy 60 (2) (2001) 129–141.
[22] E.A. Ofudje, I.A. Adeogun, M.A. Idowu, S.O. Kareem, N.A. Ndukwe, Simultaneous removals of cadmium(II) ions and reactive yellow 4 dye from aqueous solution by bone meal-derived apatite: kinetics, equilibrium and thermodynamic evaluations, Journal of Analytical Science and Technology 11 (1) (2020) 7.
[23] G. Sharma, M. Naushad, Adsorptive removal of noxious cadmium ions from aqueous medium using activated carbon/zirconium oxide composite: Isotherm and kinetic modelling, Journal of Molecular Liquids 310 (2020) 113025.
[24] G.Z. Kyzas, K.A. Matis, Nanoadsorbents for pollutants removal: A review, J. Mol. Liq. 203 (2015) 159–168.
[25] E. Deliyanni, T.J. Bandosz, K.A. Matis, Impregnation of activated carbon by iron oxyhydroxide and its effect on arsenate removal, Journal of Chemical Technology and Biotechnology 88 (6) (2013) 1058–1066.
[26] D.D. Asouhidou, K.S. Triantafyllidis, N.K. Lazaridis, K.A. Matis, S.S. Kim, T.J. Pinnavaia, Sorption of reactive dyes from aqueous solutions by ordered hexagonal and disordered mesoporous carbons, Microporous and Mesoporous Materials 117 (1-2) (2009) 257–267.
[27] E.A. Deliyanni, N.K. Lazaridis, K.A. Matis, Arsenates Sorption by Nanocrystalline Hybrid Surfactant-Akaganéite, Separation Science and Technology (Philadelphia) 47 (16) (2012) 2331–2339.
[28] A.C. Arampatzidou, D. Voutsa, E.A. Deliyanni, K.A. Matis, Adsorption of endocrine disruptor bisphenol A by carbonaceous materials: Influence of their porosity and specific surface area, Desalination and Water Treatment 76 (2017) 232–240.
[29] P.L. Yap, T.T. Tung, S. Kabiri, N. Matulick, D.N.H. Tran, D. Losic, Polyamine–modified reduced graphene oxide: A new and cost-effective adsorbent for efficient removal of mercury in waters, Separation and Purification Technology 238 (2020) 116441.
[30] Z.H. Khan, M. Gao, W. Qiu, M.S. Islam, Z. Song, Mechanisms for cadmium adsorption by magnetic biochar composites in an aqueous solution, Chemosphere 246 (2020) 125701.
[31] A.I. Zouboulis, K.A. Matis, Removal of metal ions from dilute solutions by sorptive flotation, Crit. Rev. Environ. Sci. Technol. 27 (3) (1997) 195–235.
[32] Karapantsios, T. D.; Loukidou, M. X.; Matis, K. A., Sorption Kinetics. 2005.
[33] A.G. Ritchie, Alternative to the Elovich equation for the kinetics of adsorption of gases on solids, Journal of the Chemical Society, Faraday Transactions 1: Physical Chemistry in Condensed Phases 73 (1977) 1650–1653.
[34] Y.S. Ho, J.C.Y. Ng, G. McKay, Kinetics of pollutant sorption by biosorbents: Review, Separation and Purification Methods 29 (2) (2000) 189–232.
[35] C.W. Cheung, J.F. Porter, G. McKay, Sorption kinetic analysis for the removal of cadmium ions from effluents using bone char, Water Research 35 (3) (2001) 605–612.
[36] M.S. Dzul Erosa, T.I. Saucedo Medina, R. Navarro Mendoza, M. Avila Rodriguez, E. Guibal, Cadmium sorption on chitosan sorbents: Kinetic and equilibrium studies, Hydrometallurgy 61 (3) (2001) 157–167.
[37] P.R. Puranik, J.M. Modak, K.M. Paknikar, Comparative study of the mass transfer kinetics of metal biosorption by microbial biomass, Hydrometallurgy 52 (2) (1999) 189–197.
[38] E.H. Smith, Uptake of heavy metals in batch systems by a recycled iron-bearing material, Water Research 30 (10) (1996) 2424–2434.
[39] J.S.a.P. Bendar, G. A., Random Data: Analysis and Measurement Procedures, Wiley, New York, 1986.
[40] M.X. Loukidou, T.D. Karapantsios, A.I. Zouboulis, K.A. Matis, Diffusion Kinetic Study of Chromium(VI) Biosorption by Aeromonas caviae, Industrial & Engineering Chemistry Research 43 (7) (2004) 1748–1755.
[41] Charles G. Hill, T.W. R., Introduction to Chemical Engineering Kinetics and Reactor Design, Wiley, New York, 1977.
[42] M. Loukidou, T. Karapantsios, A. Zouboulis, K. Matis, Diffusion Kinetic Study of Chromium(VI) Biosorption by Aeromonas caviae, Industrial & Engineering Chemistry Research (2004) 43.
[43] M.X. Loukidou, M.X. Λουκίδου, T.D. Karapantsios, A. Zouboulis, K.A, M.; Καραπάντσιος, Θ. Δ.; Ζουμπούλης, A. I.; Μάτης, K. A., Cadmium(II) Biosorption by Aeromonas caviae: Kinetic Modeling, Separation Science and Technology (2005) 40.
[44] C. Tien, Adsorption calculations and modeling, Butterworth-Heinemann, Boston, 1994.

[45] N.K. Lazaridis, D.D. Asouhidou, Kinetics of sorptive removal of chromium(VI) from aqueous solutions by calcined Mg-Al-CO3 hydrotalcite, Water Res 37 (12) (2003) 2875–2882.
[46] C.B. Gupt, S. Bordoloi, S. Sekharan, A.K. Sarmah, Adsorption characteristics of Barmer bentonite for hazardous waste containment application, Journal of Hazardous Materials (2020) 396.
[47] X. Jia, J. Zhou, J. Liu, P. Liu, L. Yu, B. Wen, Y. Feng, The antimony sorption and transport mechanisms in removal experiment by Mn-coated biochar, Science of The Total Environment (2020) 724.
[48] G. Kyzas, E. Deliyanni, S. Bele, K. Matis, in: Nano-Adsorbent for Arsenates: Iron Oxyhydroxide Impregnated Microporous Activated Carbon, 1, Current Environmental Engineeiring, 2014, pp. 51–58.
[49] E. Deliyanni, A. Arabatzidou, N. Tzoupanos, K. Matis, Adsorption of Pb2+ using mesoporous activated carbon and its effects on surface modifications, Adsorption Science and Technology 30 (7) (2012) 627–645.
[50] Y. Thi Dang, H.T. Hoang, H.C. Dong, K.B.T. Bui, L.H.T. Nguyen, T.B. Phan, Y. Kawazoe, T.L.H. Doan, Microwave-assisted synthesis of nano Hf- and Zr-based metal-organic frameworks for enhancement of curcumin adsorption, Microporous and Mesoporous Materials (2020) 298.
[51] D. Chen, X. Wang, K. Feng, J. Su, J. Dong, The mechanism of cadmium sorption by sulphur-modified wheat straw biochar and its application cadmium-contaminated soil, Science of The Total Environment (2020) 714.
[52] G.Z. Kyzas, N.K. Lazaridis, A.C. Mitropoulos, Removal of dyes from aqueous solutions with untreated coffee residues as potential low-cost adsorbents: Equilibrium, reuse and thermodynamic approach, Chem. Eng. J. 189-190 (2012) 148–159.
[53] G.Z. Kyzas, A decolorization technique with spent "Greek coffee" grounds as zero-cost adsorbents for industrial textile wastewaters, Materials 5 (11) (2012) 2069–2087.
[54] G.Z. Kyzas, Commercial coffee wastes as materials for adsorption of heavy metals from aqueous solutions, Materials 5 (10) (2012) 1826–1840.
[55] N.A. Travlou, G.Z. Kyzas, N.K. Lazaridis, E.A. Deliyanni, Functionalization of graphite oxide with magnetic chitosan for the preparation of a nanocomposite dye adsorbent, Langmuir 29 (5) (2013) 1657–1668.
[56] D.A. Gkika, N. Vordos, E.V. Liakos, L. Magafas, D.V. Bandekas, A.C. Mitropoulos, G.Z. Kyzas, The impact of raw materials cost on the adsorption process, Interface Science and Technology 30 (2019) 1–14.
[57] D. Gkika, E.V. Liakos, N. Vordos, C. Kontogoulidou, L. Magafas, D.N. Bikiaris, D.V. Bandekas, A.C. Mitropoulos, G.Z. Kyzas, Cost estimation of polymeric adsorbents, Polymers 11 (5) (2019).
[58] G.Z. Kyzas, E.A. Deliyanni, K.A. Matis, Activated carbons produced by pyrolysis of waste potato peels: Cobalt ions removal by adsorption, Colloids and Surfaces A: Physicochemical and Engineering Aspects 490 (2016) 74–83.
[59] M. Zhang, P. Gu, S. Yan, Y. Liu, G. Zhang, Effective removal of radioactive cobalt from aqueous solution by a layered metal sulfide adsorbent: Mechanism, adsorption performance, and practical application, Separation and Purification Technology 256 (2021) 117775.
[60] E.A. Abdelrahman, Y.G. Abou El-Reash, H.M. Youssef, Y.H. Kotp, R.M. Hegazey, Utilization of rice husk and waste aluminum cans for the synthesis of some nanosized zeolite, zeolite/zeolite, and geopolymer/zeolite products for the efficient removal of Co(II), Cu(II), and Zn(II) ions from aqueous media, Journal of Hazardous Materials 401 (2021) 123813.
[61] V.I. Mikhaylov, T.P. Maslennikova, P.V. Krivoshapkin, Characterization and sorption properties of γ-AlOOH/α-Fe2O3 composite powders prepared via hydrothermal method, Materials Chemistry and Physics 186 (2017) 612–619.
[62] J. Qu, Y. Wang, X. Tian, Z. Jiang, F. Deng, Y. Tao, Q. Jiang, L. Wang, Y. Zhang, KOH-activated porous biochar with high specific surface area for adsorptive removal of chromium (VI) and naphthalene from water: Affecting factors, mechanisms and reusability exploration, Journal of Hazardous Materials 401 (2021) 123292.
[63] E. Ben Khalifa, B. Rzig, R. Chakroun, H. Nouagui, B. Hamrouni, in: Application of response surface methodology for chromium removal by adsorption on low–cost biosorbent, 189, Chemometrics and Intelligent Laboratory Systems, 2019, pp. 18–26.
[64] C.-A. Ghiorghita, K.B.L. Borchert, A.-L. Vasiliu, M.-M. Zaharia, D. Schwarz, M. Mihai, Porous thiourea-grafted-chitosan hydrogels: Synthesis and sorption of toxic metal ions from contaminated waters, Colloids and Surfaces A: Physicochemical and Engineering Aspects 607 (2020) 125504.
[65] E. Aboli, D. Jafari, H. Esmaeili, Heavy metal ions (lead, cobalt, and nickel) biosorption from aqueous solution onto activated carbon prepared from Citrus limetta leaves, Carbon Letters 30 (6) (2020) 683–698.
[66] S.S.G. Santos, D.B. França, L.R.C. Castellano, P. Trigueiro, E.C. Silva Filho, I.M.G. Santos, M.G. Fonseca, Novel modified bentonites applied to the removal of an anionic azo-dye from aqueous solution, Colloids and Surfaces A: Physicochemical and Engineering Aspects 585 (2020) 124152.
[67] K.C. Bedin, S.P. de Azevedo, P.K.T. Leandro, A.L. Cazetta, V.C. Almeida, Bone char prepared by CO2 atmosphere: Preparation optimization and adsorption studies of Remazol Brilliant Blue R, Journal of Cleaner Production 161 (2017) 288–298.
[68] D.F. Brito, E.C. da Silva Filho, M.G. Fonseca, M. Jaber, Organophilic bentonites obtained by microwave heating as adsorbents for anionic dyes, Journal of Environmental Chemical Engineering 6 (6) (2018) 7080–7090.
[69] S. Lawchoochaisakul, P. Monvisade, P. Siriphannon, Cationic starch intercalated montmorillonite nanocomposites as natural based adsorbent for dye removal, Carbohydrate Polymers 253 (2021) 117230.
[70] L.R. Bonetto, J.S. Crespo, R. Guégan, V.I. Esteves, M. Giovanela, Removal of methylene blue from aqueous solutions using a solid residue of the apple juice industry: Full factorial design, equilibrium, thermodynamics and kinetics aspects, Journal of Molecular Structure 1224 (2021) 129296.
[71] P. De Luca, J.B. Nagy, Treatment of water contaminated with reactive black-5 dye by carbon nanotubes, Materials 13 (23) (2020) 1–19.
[72] J.C. Coura, D. Profeti, L.P.R. Profeti, Eco-friendly chitosan/quartzite composite as adsorbent for dye removal, Materials Chemistry and Physics (2020) 256.
[73] K.C. Lai, L.Y. Lee, B.Y.Z. Hiew, T.C.-K. Yang, G.-T. Pan, S. Thangalazhy-Gopakumar, S. Gan, Utilisation of eco-friendly and low cost 3D graphene-based composite for treatment of aqueous Reactive Black 5 dye: Characterisation, adsorption mechanism and recyclability studies, Journal of the Taiwan Institute of Chemical Engineers 114 (2020) 57–66.
[74] S. Wong, N.A. Ghafar, N. Ngadi, F.A. Razmi, I.M. Inuwa, R. Mat, N.A.S. Amin, Effective removal of anionic textile dyes using adsorbent synthesized from coffee waste, Scientific Reports 10 (1) (2020).